9

Dawid Kwaśniak and Marcin Uradziński\*

# The usefulness of the MAFA method for smartphone precise positioning

https://doi.org/10.1515/jag-2025-0008 Received January 20, 2025; accepted April 1, 2025; published online April 23, 2025

**Abstract:** The paper presents smartphone GPS positioning results, using phase observations on the L1 frequency. In this research, we used one Huawei P30 Pro mobile phone, one Samsung S22 Ultra, and one geodetic receiver (Javad Triumph-1) acting as the reference receiver. Smartphones were placed on an aluminum base at an equal distance of 0.34 m from this receiver. Such a close distance was used to achieve identical observation conditions. The analysis was carried out from static GPS positioning, using the Modified Ambiguity Function Approach (MAFA) method. The short baselines were used during the tests. For the first part of the test, 5-min static sessions were performed for both smartphones. For post-processing kinematic (PPK), 1, 3, 5, and 10-s solutions achieved decimeter-level accuracy, while 30 and 60-s solutions provided centimeter-level accuracy for N and E on both smartphones. The results obtained from both smartphones are very promising. The authors proved that the MAFA method can be used for precise mobile phone positioning for short baselines.

**Keywords:** smartphone positioning; MAFA method; GNSS; phase measurements

#### 1 Introduction

The usefulness of Global positioning system (GPS) phase measurements has been known since the beginning of satellite positioning. These first measurements depended mainly on L1 and L2 frequencies, available in every high-class GPS receiver and broadcasted by all currently operational satellites. Nowadays, the phase observations on additional L5 frequency provide more applicability. The GPS L5 signal is one of the latest signals related to the GPS modernization

plan. The L5 signal operates at a higher power level than other civilian GPS signals, features a broader bandwidth, and transmits at a lower frequency, enhancing its reception for indoor positioning applications [1]. Furthermore, integrating multiple satellite systems, including GLONASS, Galileo, and BeiDou, into modern smartphones has greatly enhanced the precision and reliability of positioning services.

Since phase observations were applied to smartphones, they have emerged as a valuable tool for precision positioning, transforming the capabilities of everyday mobile devices for a wide range of applications. Traditionally, carrier phase measurements have been the domain of high-end GNSS receivers, relied upon in fields such as surveying, geodesy, and autonomous navigation. Today, smartphone-based Global Satellite Navigation System (GNSS) technology may play an influential role in these areas, as well as in earthquake warnings and environmental monitoring [2–4].

Recent advancements in smartphone technology have made it possible to access raw GNSS measurements through the new application programming interface (API) [5]. However, the new API does not provide the typical GNSS observations directly (e.g., pseudorange, carrier-phase, or Doppler observations), which have to be generated by the users themselves to obtain a high level of accuracy under optimal conditions. This development opens a vast array of possibilities for applications that require high-precision location data but were previously constrained by the limitations of standard GNSS position fixes on mobile devices. High-precision positioning on smartphones, accurate to the decimeter and even centimeter levels, has attracted considerable attention [6–10]. To achieve centimeter-level positioning using smartphone GNSS data, it is crucial to assess the quality of the raw measurements. Accurate evaluation begins with the proper acquisition, conversion, and processing of GNSS observations. Receiver Independent Exchange Format (RINEX) is widely used by scientists for its compatibility with established GNSS processing tools. Smartphone GNSS data logging is facilitated by specialized applications that capture raw sensor observations. The Geo++ RINEX Logger (https://www.geopp.de), a pioneering application, was the first to directly convert raw GNSS observables from the Android API into RINEX files, making them compatible with conventional GNSS processing frameworks. This tool

E-mail: marcin.uradzinski@uwm.edu.pl. https://orcid.org/0000-0002-5934-8293

**Dawid Kwaśniak**, Faculty of Geoengineering, University of Warmia and Mazury, 10-720 Olsztyn, Poland

<sup>\*</sup>Corresponding author: Marcin Uradziński, Faculty of Geoengineering, University of Warmia and Mazury, 10-720 Olsztyn, Poland, E-mail: marcin.uradzinski@uwm.edu.pl. https://orcid.org/0000-0002-

remains the most widely adopted for logging raw GNSS data from smartphones [11]. Also, the growing support for dualfrequency GNSS measurements in modern smartphones represents a significant advancement. Additional frequencies enhance measurement precision and help mitigate multipath distortions. Such capabilities, combined with robust logging and processing tools, pave the way for achieving higher levels of accuracy and reliability in smartphone GNSS applications.

Incorporating phase observations into GNSS positioning systems offers several compelling advantages, particularly in achieving higher accuracy and stability compared to traditional code-based solutions. This is especially valuable in challenging environments such as urban areas or locations with significant signal obstructions, where code-based methods often struggle. Phase-based positioning leverages the precise measurement of the carrier wave's phase, enabling the resolution of smaller positional changes and improved reliability. Notably, achieving centimeterlevel accuracy is no longer confined to high-end specialized equipment. Recent advancements demonstrate the feasibility of using single-frequency carrier-phase differential GNSS techniques with consumer-grade smartphone hardware for static positioning scenarios [11, 12]. These methods capitalize on the raw carrier-phase data provided by modern smartphones, combining it with advanced processing algorithms to deliver remarkable precision. Also, available today lowcost positioning modules, e.g., u-blox, set the benchmark in high precision GNSS performance. The latest developments have made high-accuracy GNSS positioning more accessible for everyday use [8]. Research shows that singlefrequency smartphone-based techniques like RTK, and network RTK (NRTK) can achieve mostly decimeter-level accuracy under optimal conditions [13–17]. While studies have demonstrated the potential of smartphones to deliver accurate positioning, these advancements rely on advanced algorithms and satellite communication technologies. Despite this progress, achieving consistent high-accuracy positioning remains dependent on favorable conditions.

Furthermore, researchers have increasingly explored the application of precise point positioning (PPP) techniques to smartphones, marking a transformative step in location technology [18]. Initial efforts in applying PPP to smartphones focused on single-frequency PPP static experiments, yielding decimeter-level accuracy under ideal conditions [19]. Also, real-time solutions represent a major step forward, extending PPP's benefits to dynamic applications where positional information is critical [20, 21]. A particularly promising evolution of this technique is Precise Point Positioning with Ambiguity Resolution (PPP-AR). Despite many advancements, the effectiveness of PPP and PPP-AR heavily depends on the quality of GNSS signals. Environments with significant signal obstructions, such as urban areas with dense buildings or heavily forested regions, can impair performance. The multipath effect, signal attenuation, and loss of satellite visibility in such scenarios remain key challenges that researchers actively address through algorithmic improvements and sensor integration techniques [22, 23]. Another technique like PPP-RTK has been extensively studied for its ability to combine the benefits of both real-time kinematic RTK and PPP techniques. Before the development of PPP-RTK, traditional RTK relied on a single base station, but it was later extended to work within a regional network of multiple base stations, referred to NRTK. RTK and NRTK allow for rapid ambiguity resolution over short baselines or within a local area. In contrast, PPP eliminates the need for a local network like NRTK, operating with just a single receiver. However, PPP typically faces longer convergence times for ambiguity resolution. PPP-RTK, therefore, offers the fast ambiguity resolution capabilities of RTK and NRTK while overcoming the convergence delay associated with standalone PPP [24].

The MAFA method (Modified Ambiguity Function Approach) presented by the authors is based on the alignment using the least squares method with conditional equations in the functional model [25]. The use of conditional equations allows for the elimination of phase observation ambiguity from the mathematical model underlying the adjustment process while simultaneously taking into account the integer nature of these ambiguities in the obtained solutions. In comparison to the modern positioning methods, the MAFA method is unaffected by cycle slips and discontinuity of ambiguities [26]. The MAFA method is based on relative positioning. In the case of the MAFA method, there is no need to remove the cycle slips, thanks to the mathematical models. While considering the classical models of ambiguity resolutions, if the satellite observations are missing even for one epoch, the ambiguities will change. Such a problem does not exist in the MAFA method, thanks to the search procedure incorporated into this method [27].

Despite substantial progress in smartphone GNSS technology, unfortunately, several critical limitations continue to impede its effectiveness in high-precision applications. A key challenge is the presence of noisy or inconsistent measurements, which significantly impact the reliability and accuracy of GNSS data. These issues largely stem from the limitations of smartphone hardware, particularly the use of compact, low-quality GNSS antennas. Unlike the high-gain, circularly polarized antennas used in professional equipment, smartphone antennas are constrained by

design priorities such as size, cost, and integration with other components. As a result, they are more susceptible to interference, multipath effects, and weak signal reception [28]. The compact form factor of smartphones further exacerbates these issues, as the antenna's proximity to other internal components, such as metal casings and electronic circuits, introduces additional noise and signal distortion. To address these challenges, researchers are exploring several avenues. One approach involves the development of advanced signal processing algorithms to mitigate noise and improve measurement quality. For example, techniques such as multipath filtering, machine learning-based error correction, and real-time signal enhancement have shown promise in improving GNSS accuracy [22]. Another area of focus is the design of improved smartphone antennas, including multi-band and multi-polarization configurations, to enhance signal reception and reduce susceptibility

Additionally, the integration of GNSS data with information from other sensors (accelerometers, gyroscopes, or barometers) can provide complementary positioning data, improving overall accuracy and reliability [29, 30]. Collaborative techniques like assisted GNSS (A-GNSS), which leverages network-based corrections, also help mitigate the shortcomings of smartphone hardware in challenging environments [31]. While these advancements represent significant progress, achieving consistent centimeterlevel accuracy across diverse environments remains a formidable challenge. Continued innovation in hardware design, algorithm development, and hybrid positioning solutions will be essential to unlock the full potential of smartphone GNSS for precise applications.

### 2 MAFA method

The MAFA method is based on relative positioning. We can present the double-differenced phase observations equation in a simplified form. For our considerations, we will ignore the influence of the troposphere and ionosphere (however, they can be modeled and included in the model) [32]:

$$\Phi = \frac{1}{\lambda} \rho(\mathbf{x}_c) + N + e \tag{1}$$

where:  $\Phi$  – double-differenced phase observations;  $\lambda$  – wave length;  $\rho$  – double-differenced geometric distances; N – double-differenced ambiguities; e – observation errors (measurement noise);  $\mathbf{x}_c$  – coordinates vector of the receiver. The nominal accuracy of phase observation measurements is typically determined at approximately 0.01 cycles. This means the corrections should be considerably

less than 0.5 cycles of the measured phase [33]. Considering the integer nature of the parameter N and assuming that errors are less than half a cycle we can present equation (1) in the following form [34]:

$$e = \left(\Phi - \frac{1}{\lambda}\rho(\mathbf{x}_c)\right) - \operatorname{int}\left(\Phi - \frac{1}{\lambda}\rho(\mathbf{x}_c)\right)$$
 (2)

where "int" denotes rounding to the nearest integer. The term int  $\left(\Phi - \frac{1}{2}\rho(\mathbf{x}_c)\right)$  in equation (2) has been introduced in place of the element N. This can be made only if two conditions are fulfilled. The first one has been already introduced that the corrections should be considerably less than half of the cycle. The second condition pertains to the approximate value of  $\mathbf{x}_c$ . The approximate value of the position must lie within the appropriate region called the Voronoi cell [35] or pull-in region [36]. The fulfilment of the second condition is ensured through a search procedure described in the later part of this paper. The linearized form of equation (2) can be presented as follows [34]:

$$\mathbf{e} = \mathbf{\delta} - \frac{1}{\lambda} \mathbf{A} \mathbf{d} \mathbf{x}_{\mathbf{c}} \tag{3}$$

where  $\mathbf{dx}_{\mathbf{c}}$  – is a parameter vector,  $\mathbf{A}$  – is the design matrix, e – is the error vector and  $\delta$  – is the misclosures vector, which is formed in the presented form:

$$\delta = \left(\mathbf{\Phi} - \frac{1}{\lambda}\rho(\mathbf{x}_c^0)\right) - \operatorname{int}\left(\mathbf{\Phi} - \frac{1}{\lambda}\rho(\mathbf{x}_c^0)\right)$$
(4)

where  $\rho(\mathbf{x}_c^0)$  is a vector of double-differenced geometric distances calculated using approximate coordinates, there are no ambiguities in the presented model (3). However, its integer nature is preserved through the appropriate formula for creating the misclosures vector (4). By adopting this approach, the least-squares adjustment problem with integer constraints transforms into the unconstrained form represented by the model in equation (3) and the corresponding objective function:

$$\Psi = \mathbf{e}^T \mathbf{P} \mathbf{e} \tag{5}$$

where P in this equation is a weight matrix. Utilizing the least-squares method allows us to determine  $dx_c$  and e:

$$\widetilde{\mathbf{dx}}_c = \lambda (\mathbf{A}^T \mathbf{P} \mathbf{A})^{-1} \mathbf{A}^T \mathbf{P} \boldsymbol{\delta}$$
 (6)

$$e = \delta - \frac{1}{\lambda} A d x_c$$
 (7)

The presented solution (6) obtained from the model (3) is correct when the a priori position lies within the appropriate Voronoi cell [35]. However, only in some cases, this will work. Hence, introducing a search procedure becomes necessary in the MAFA method. In the MAFA method, the

search procedure is conducted in the 3-dimensional domain of x, y, z coordinates. The search region is created as an ellipse of errors of approximate position. A grid of optimally distributed points called candidates is created within it. The orientation of a grid aligns with the orientation of the axes of the error ellipse. The density of the candidate grid must be dense enough not to miss the correct Voronoi cell, but at the same time, it cannot be too dense. The large number of candidates to test can make the computation process ineffective [37]. The confidence level determines the size of the error ellipsoid. The parameters describing the error ellipsoid are the centre, the lengths of the main axes, and their orientation [27]. Those parameters are determined based on the vector of the approximate position and the covariance matrix  $Q_x$  of this position. To determine the length of the axis of the error ellipsoid, we must use the relationship between the critical value  $\chi_c^2$  of the  $\chi^2$  distribution with 3 degrees of freedom and the assumed confidence level  $p_0$ [31]:

$$p_0 = P(\chi^2 < \chi_c^2) \tag{8}$$

where:

$$\chi^2 = (\mathbf{x}_c - \mathbf{x}_c^0)^{\mathsf{T}} \mathbf{Q}_{\mathbf{x}}^{-1} (\mathbf{x}_c - \mathbf{x}_c^0)$$
 (9)

In this paper the confidence level  $p_0$  was set as 0.6. With equation (9) we can write  $\chi^2 < \chi_c^2$  from (8) as:

$$(\mathbf{x}_{c} - \mathbf{x}_{c}^{0})^{\mathrm{T}} \mathbf{Q}_{\mathbf{x}}^{-1} (\mathbf{x}_{c} - \mathbf{x}_{c}^{0}) < \chi_{c}^{2}$$
 (10)

This inequality defines a confidence region adopted as the search region. The centre of the error ellipse is set at the *a priori* point, and the length of the main axis of the error ellipse is determined in the following way:

$$r_{x} = \sqrt{\frac{\chi_{c}^{2}}{\mu_{x}}}, r_{y} = \sqrt{\frac{\chi_{c}^{2}}{\mu_{y}}}, r_{z} = \sqrt{\frac{\chi_{c}^{2}}{\mu_{z}}}$$
 (11)

where  $\chi_{\mathbf{c}}^2$  a critical value of  $\chi^2$  distribution with 3 degrees of freedom.  $\mu_{\mathbf{x}}$ ,  $\mu_{\mathbf{y}}$ ,  $\mu_{\mathbf{z}}$  are eigenvalues of the matrix  $\mathbf{Q}_{\mathbf{x}}^{-1}$ .

When the grid of candidates is prepared, each of them is tested. Each is set as an approximate position, and the criteria (5) is tested. The candidate that minimizes the criteria is accepted as the solution. The estimation using this candidate is performed, and the results are taken as a final result for the MAFA method.

In the MAFA method for smartphone positioning, cycle slips do not need to be removed, thanks to the mathematical model. This simplifies the data preparation. In contrast, traditional ambiguity resolution models are affected by missing satellite observations – just one lost epoch can alter the ambiguities. This issue is avoided in the MAFA method due to the search procedure built into it. This method allows us

to obtain a position from one epoch solution, which is very desirable in mobile device positioning.

# 3 Field experiment and configuration

Experiments were conducted in the open-sky area. The tests were done for a chosen period of 60 min (recording interval – 1s) in static mode. Raw GNSS observation data was collected using Geo++ Rinex Logger Android application ver. 2.1.8 by Huawei P30 Pro and Samsung S22 Ultra smartphones. These mobile phones collect data from GPS, GLONASS, BEIDOU, and GALILEO positioning systems. Huawei P30 Pro uses Kirin 980 chipset, and the Samsung S22 Ultra uses Qualcomm SM8450 Snapdragon 8 Gen 1 chipset.

Additionally, in this research, we used a geodetic receiver (Javad Triumph-1) acting as the reference receiver. Smartphones were placed at an equal distance of 0.34 m from this receiver (Figure 1). The authors specially planned such a close distance to achieve identical observation conditions. Thus, it was possible to compare the accuracy of MAFA/GPS positioning using phase observations on the L1 frequency.

To achieve the highest level of accuracy in positioning, precise knowledge of the average phase center position of the smartphone's internal antenna – as well as any potential variations in that phase center – is essential [7, 8]. Before initiating the main positioning accuracy experiment, we conducted two preliminary sessions, each lasting 2 h, to determine the phase center. In these following



Figure 1: Field experiment and equipment configuration.

sessions, smartphones were mounted separately on a specially constructed aluminum base, designed with a centrally positioned mandrel that allowed for secure placement on a leveling head. This setup ensured precise alignment over a designated reference point. To explore the impact of orientation on the phase center, the smartphones were fixed in three distinct positions on the aluminum base: (1) vertically upright, (2) lying parallel to the length of the beam, and (3) positioned perpendicular to the beam. Simultaneously, two high-precision GNSS Javad Alpha receivers were mounted at the North and South ends of the aluminum base. The setup included a professional-grade compass, which facilitated the exact alignment of the base along the North-South axis. Carrier phase measurements from each setup were recorded and subsequently processed using Topcon Tools, a commercial post-processing software. For accurate differential positioning, data from the nearest ASG-EUPOS (Polish GNSS augmentation system) base station, located 4 km away, served as the reference in the post-processing step for antenna phase center determination. This setup allowed for a comprehensive assessment of potential phase center shifts in various smartphone orientations, providing essential calibration data to enhance the reliability of subsequent positioning accuracy experiments. Knowing the placement of phase centers of both smartphones, we could measure the exact distances to the Javad receiver for comparison purposes. More detailed information about the calibration of Huawei's smartphone antenna's phase center with its precise localization can be found in [9]. The similar results were obtained by Wanninger and Heßelbarth in [8]. According to Samsung's phase center calibration process and final parameters can be found in [38].

All the computations were performed using a self-made by authors software in MatLab. The software uses the MAFA method for positioning using code and phase observations. The software can perform computations in two modes: static sessions and post-processed kinematics (PPK). These two modes were used in the presented tests. In both cases, the reference station is required to perform the computations. The confidence level was set as 0.6. Many tests were performed to determine the best value for confidence level. Javad receiver was used as a reference station. The elevation mask for the calculation was 15° for both modes. The authors decided to use a short baseline since the MAFA method was never tested with low-quality observations. It was unclear if the method would be able to estimate the position with such data.

In the static mode, the results were obtained by initially determining the position for the first epoch, then subsequently incorporating observations from the next epoch, re-estimating, and repeating this process until the final epoch. As each subsequent epoch occurred, a more extensive set of observations was utilized for estimation. A similar approach was adopted for the PPK mode. However, in this case, the position was estimated using a previously assumed number of epochs. In the presented tests, the 1, 3, 5, 10, 30, and 60 s long PPK sessions were used. In the 1-s approach, data from a single epoch is used to estimate the position, while in the 60-s approach, data from 60 consecutive epochs is used. The main difference lies in the number of epochs and the data used for the estimation. For comparison purposes, the accurate position of the reference Javad Triumph-1 receiver was determined using the closest ASG-EUPOS permanent reference station (OPNT). To present the obtained results, the coordinate differences between reference coordinates and obtained results were calculated and transformed into a topocentric coordinate system. Both smartphone positions were determined using relative positioning in reference to the Javad receiver.

# 4 Positioning results and discussion

In this section, results from long static sessions and PPK are presented. For the first part of the test, 5-min static sessions were performed for both mobile phones. Initially, we used a one-hour static session. However, we decided to show only a 5-min static session because, after a few minutes, the position got stable. The authors decided not to show the rest of the positioning results since it does not present any significant changes. Figure 2 presents the results for Huawei and Samsung static sessions. The first plot of Figure 2 shows the results for Huawei. For Huawei, the position gets stable after around 25 s. After about 2 min, the position gets stable with very high accuracy.

Second plot of Figure 2 presents the results for Samsung. In this case, about 25 s were needed to obtain a stable and precise position. But as we can observe, Samsung's accuracy is lower than Huawei's. Also, after the convergence, Samsung's position became unstable. The position errors for XYZ in the last epoch for Huawei are, respectively, 0.003 m, 0.002 m, and 0.004 m. In the case of Samsung, we got 0.003 m, 0.002 m and 0.004 m. So, we can observe that position errors in both cases are similar. However, we can observe higher variability in Samsung's case than in Huawei's.

Figures 3 and 4 present the results for PPK for Huawei. We can observe very low precision for the obtained positions for the one, three, and five-epoch solutions and even for ten-second solutions. In these four types of solutions, we can observe differences between the reference and

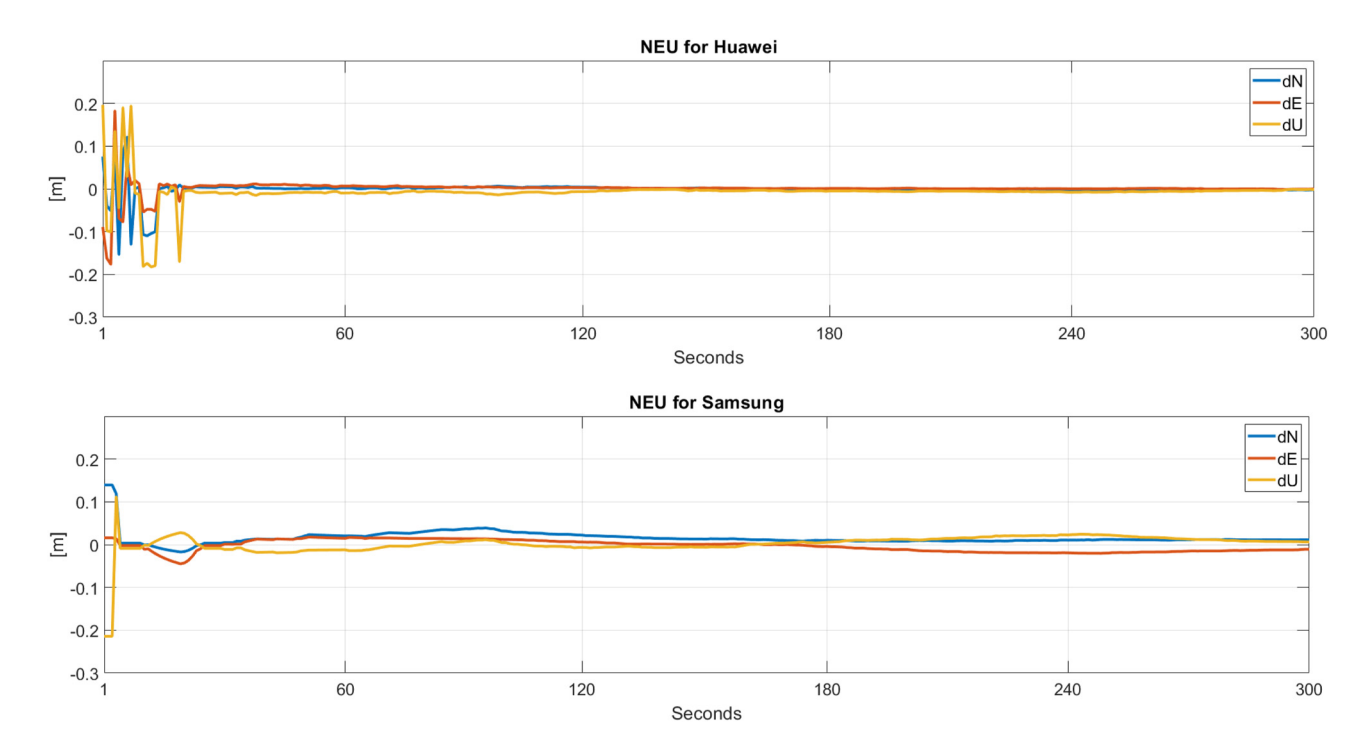


Figure 2: dN, dE and dU for Huawei and Samsung GPS-only static sessions.

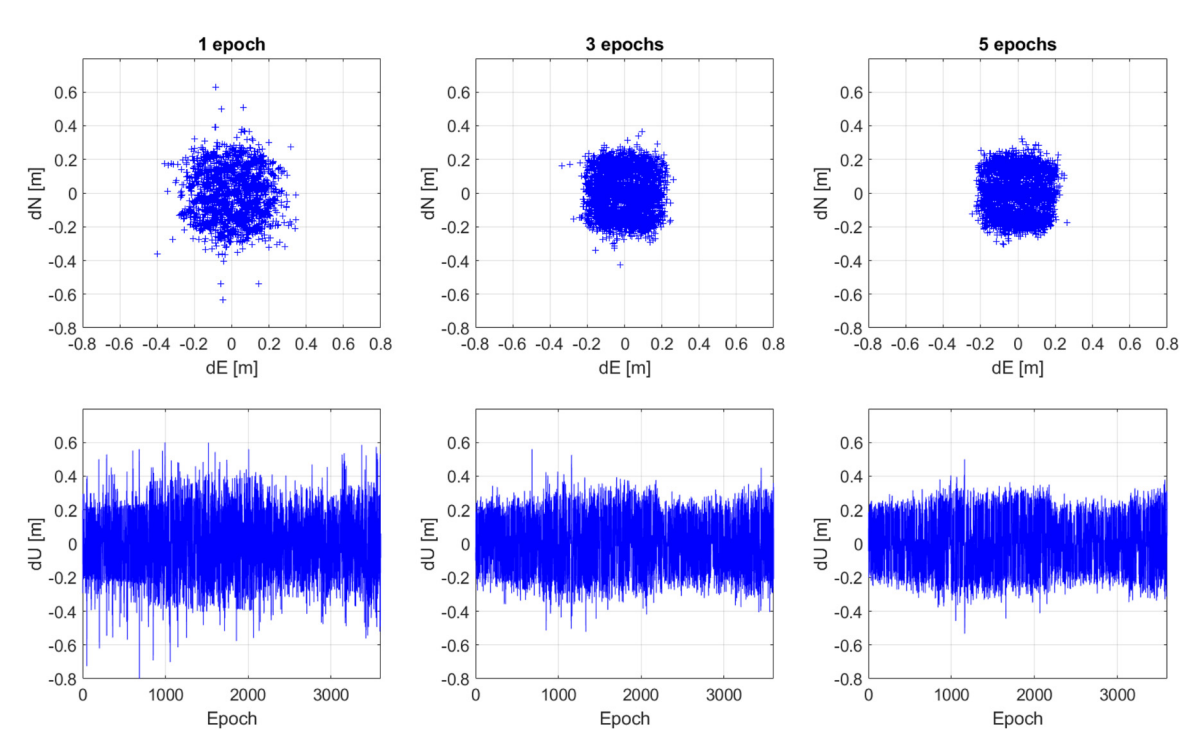


Figure 3: One, three and five epoch dN, dE and dU post-processing GPS-only PPK results for Huawei.

obtained positions that can be significantly larger than 0.2 m. Those differences are smaller than 0.2 m for 30 and 60-epoch solutions for dN and dE. In the case of dU, as expected the precision is even lower, and in all six cases. For one, three, and five-second solutions, the differences

between reference position and obtained positions can reach even 0.5 m. For ten, thirty and sixty-epochs solutions, differences reach up to  $0.3\ m.$ 

A similar situation can be observed in Figures 5 and 6, where PPK results are presented from Samsung. Also, in this

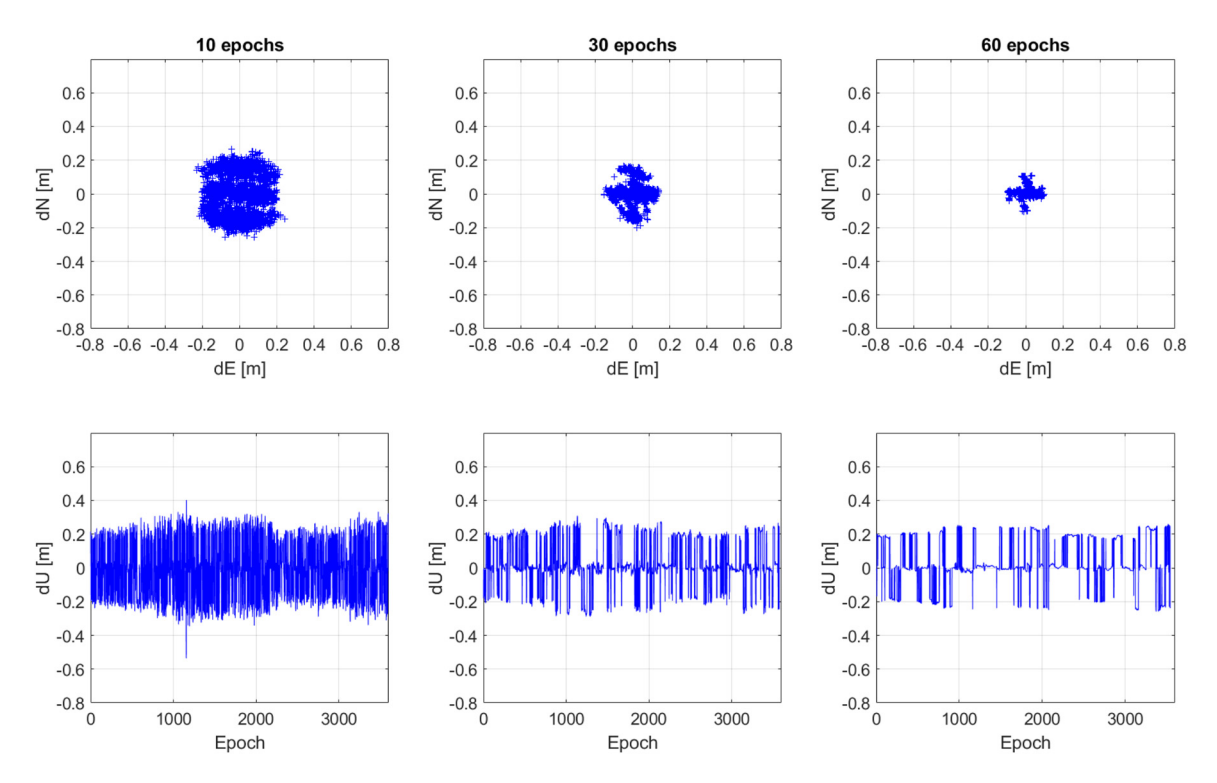


Figure 4: Ten, thirty, and sixty epoch dN, dE, and dU post-processing GPS-only PPK results for Huawei.

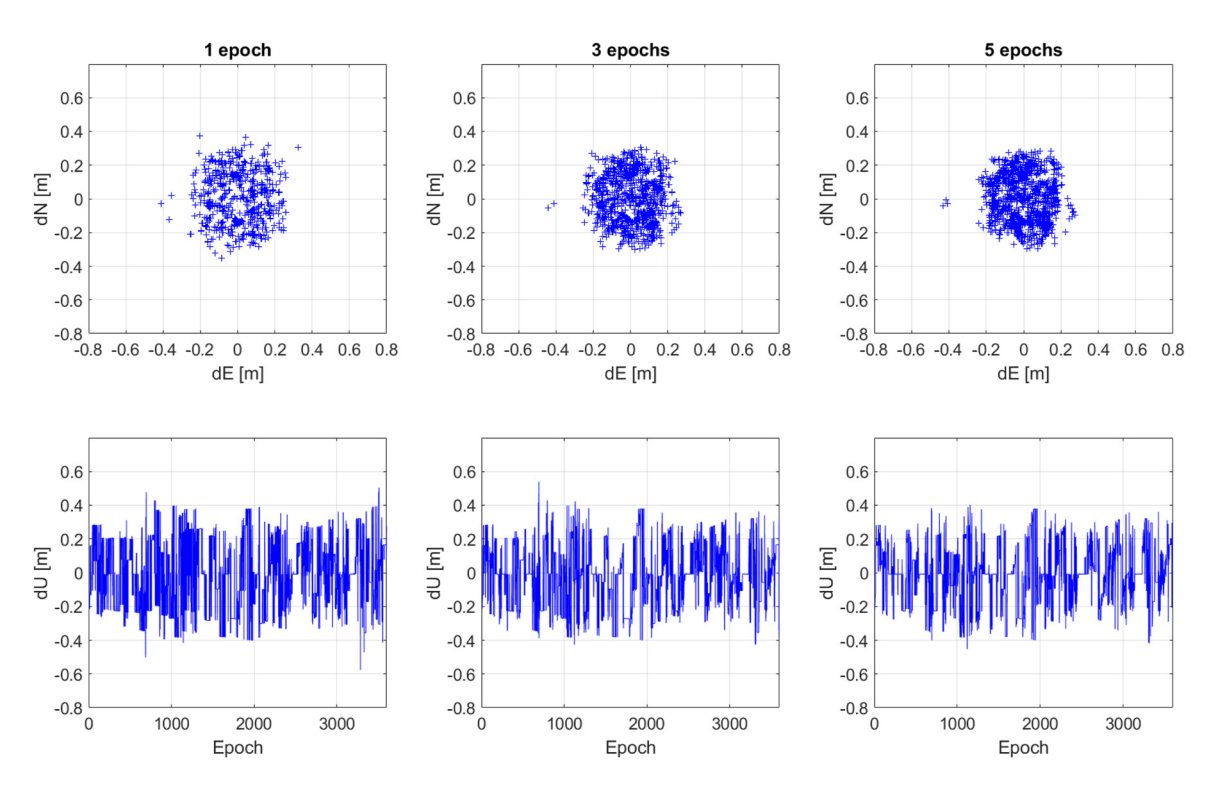


Figure 5: One, three and ten epoch dN, dE and dU post-processing GPS-only PPK results for Samsung.

case, we can observe a low accuracy for one, three, five, and ten-second solutions for dN and dE. The differences between the reference position and obtained positions can exceed

0.3~m. The results for dU are also similar. The results for the first four variants can exceed 0.3~m. For thirty and sixty-second solutions, the results are primarily below 0.3~m.

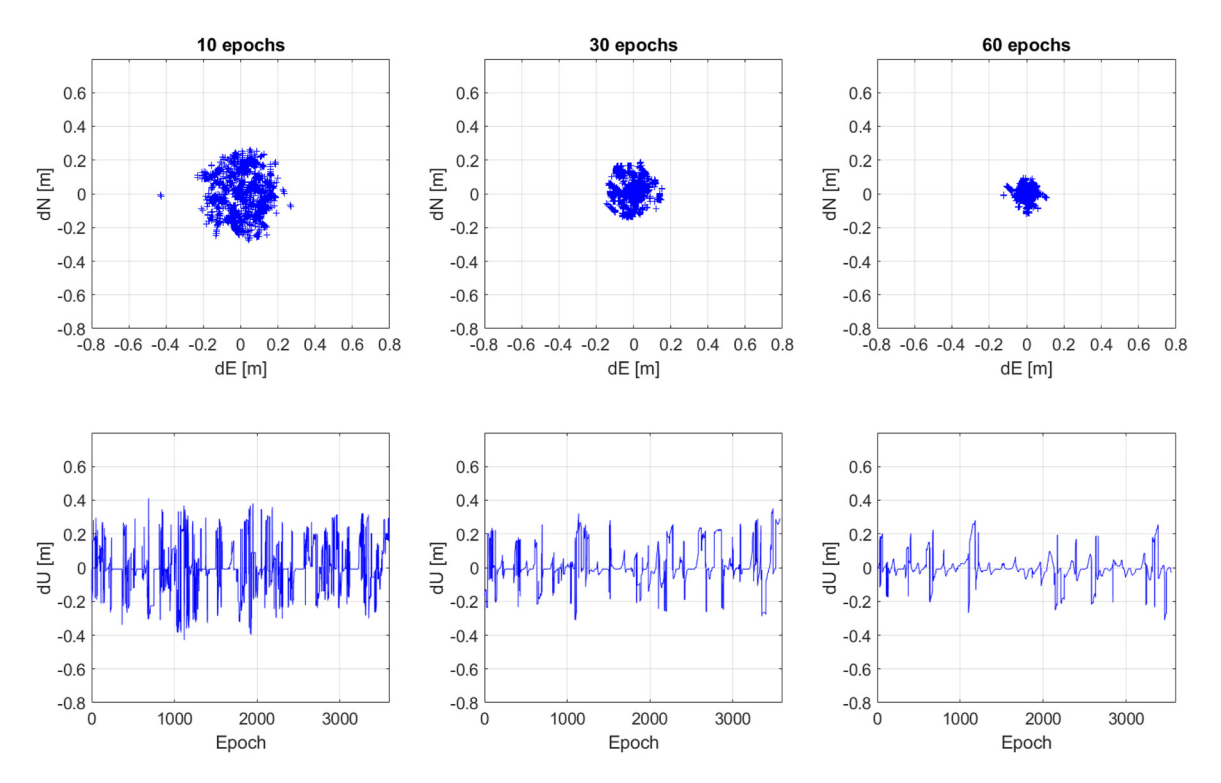


Figure 6: Ten, thirty and sixty epoch dN, dE and dU post-processing GPS-only PPK results for Samsung.

However, in the case of Samsung, we can observe that the more significant number of obtained solutions are characterized by high precision in cases of ten, thirty and sixtysecond solutions.

Table 1 presents the post-processing results for Huawei and Samsung. The mean of the differences between reference and obtained positions and the standard deviations (std) for those differences are shown. We can observe that the obtained means are close to a few millimetres for all solutions for both Samsung and Huawei. The situation differs when it comes to the standard deviation. In the case of both Samsung and Huawei, the standard deviation for one and three-epoch solutions is over 0.1 m for dN and dU. For

five and ten-second solutions, std for dN is still bigger than 0.1 m. However, for dE, it drops below 0.1 m for Samsung. For 30-s solutions for Huawei, std is just above 0.05 m, and for Samsung, it is slightly below 0.05. For 60-s solutions, the standard deviations are below 0.03 m for both Huawei and Samsung. For dU, the standard deviation for both mobile phones is over 0.2 m in a one-epoch solution. For Huawei, the value for the remaining solutions is always greater than 0.1 m. In the case of Samsung, only for a 60-s solution, std is below 0.1 m.

Based on experimental results presented by the researchers in previous scientific papers, we can observe that authors obtained a similar level of accuracy using the

Table 1: Mean and standard deviation for dN, dE, and dU for Huawei and Samsung.

Huawei												
	1 epoch		3 epochs		5 epochs		10 epochs		30 epochs		60 epochs	
	Mean	Std	Mean	Std	Mean	Std	Mean	Std	Mean	Std	Mean	Std
dN	-0.003	0.142	0.000	0.129	-0.002	0.126	-0.006	0.118	0.000	0.056	0.004	0.027
dE	-0.001	0.118	-0.001	0.105	0.001	0.103	0.002	0.096	0.009	0.051	0.006	0.026
dU	-0.001	0.217	0.001	0.190	0.001	0.188	-0.007	0.182	0.026	0.140	0.033	0.138
						Samsung						
dN	0.002	0.132	-0.002	0.122	0.000	0.114	-0.003	0.101	0.005	0.047	0.000	0.025
dE	0.012	0.108	0.010	0.101	0.007	0.095	0.004	0.081	0.000	0.040	-0.003	0.021
dU	-0.020	0.020	-0.023	0.185	-0.006	0.172	-0.001	0.147	0.013	0.112	-0.005	0.078

MAFA method in a much shorter time (after 25 s) using GPS L1. After Wanniger and Heßelbarth, the fixed solution achieved accuracies from 3.5 cm in 5 min to 1.6 cm in 60 min using WaSoft software [8]. Uradziński and Bakuła obtained similar accuracies (1-2 cm) after 20 min using Topcon Tools software [9]. The same positioning results were obtained after 30 min using RTKLib software [39]. However, it is important to note, that the cited authors used longer baselines.

## 5 Summary and conclusions

The paper presents the GPS positioning results obtained from smartphones, using phase observations on the L1 frequency. In this research, we used one Huawei P30 Pro mobile phone, one Samsung S22 Ultra, and one geodetic receiver (Javad Triumph-1) acting as the reference receiver. The analysis was carried out from static GPS positioning, using the MAFA method.

In the first part of the test, 5-min static sessions were conducted for both mobile phones. For the Huawei smartphone, the position stabilized after approximately 25 s and achieved very high accuracy after around 2 min. For the Samsung smartphone, it also took about 25 s to obtain a stable and precise position. The position errors for XYZ in the final epoch for the Huawei device were 0.003 m, 0.002 m, and 0.004 m, respectively. For the Samsung device, the errors were 0.003 m, 0.002 m, and 0.004 m as well. Thus, the position errors in both cases are similar. However, there is greater variability in the results of Samsung compared to Huawei.

For PPK, the 1, 3, 5, and 10-s solutions show decimeterlevel accuracy, while the 30 and 60-s solutions provide centimeter-level accuracy for N and E coordinates for both smartphones. For the Up component, results were below 0.3 m. For Huawei, the STD for 1-epoch solutions was 0.12 m for dN and dE, and 0.22 m for dU. For 60-epoch solutions, the STD was 0.03 m for dN and dE, and 0.14 m for dU. Samsung's 1-epoch results were similar to Huawei's, but for the 60-epoch solution, Samsung's dN and dE were comparable to Huawei's, while dU was nearly double, at 0.07 m. In comparison to other research papers, we can observe that authors obtained a similar level of accuracy using the MAFA method in a much shorter time (after 25 s) using GPS L1 frequency.

The results obtained from both smartphones are very promising. The authors proved that the MAFA method can be used for precise mobile phone positioning for short baselines. In the near future, authors are planning to extend the MAFA method to process multi-GNSS data.

**Research ethics:** Not applicable. **Informed consent:** Not applicable.

Author contributions: All authors have accepted responsibility for the entire content of this manuscript and approved its submission.

Use of Large Language Models, AI and Machine Learning

Tools: None declared.

**Conflict of interest:** The authors state no conflict of interest.

Research funding: None declared. Data availability: Not applicable.

### References

- 1. Uradziński M, Bakuła M. Comparison of L1 and L5 GPS smartphone absolute positioning results. J Appl Geodesy 2024;18:51-68.
- 2. Alsubaie NM, Youssef AA, El-Sheimy N. Improving the accuracy of direct geo-referencing of smartphone-based mobile mapping systems using relative orientation and scene geometric constraints. Sensors 2017;17:2237.
- 3. Paziewski J. Recent advances and perspectives for positioning and applications with smartphone GNSS observations. Meas Sci Technol 2020;31:091001.
- 4. Kong Q, Allen RM, Schreier L, Kwon YW. MyShake: a smartphone seismic network for earthquake early warning and beyond. Sci Adv 2016;2:e1501055.
- 5. Zangenehnejad F, Jiang Y, Gao Y. GNSS observation generation from smartphone android location API: performance of existing apps, issues and improvement. Sensors 2023;23:777.
- 6. Li G, Geng J. Characteristics of raw multi-GNSS measurement error from Google Android smart devices. GPS Solut 2019;23:90.
- 7. Pesyna KM, Heath RW, Humphreys T. Centimeter positioning with a smartphone-quality GNSS antenna. In: Proceedings of the 27th international technical meeting of the satellite division of the institute of navigation (ION GNSS+ 2014). Tampa, FL, USA; 2014:1568 - 77 pp.
- 8. Wanninger L, Heßelbarth A. GNSS code and carrier phase observations of a Huawei P30 smartphone: quality assessment and centimeter-accurate positioning. GPS Solut 2020;24:64.
- 9. Uradziński M, Bakuła M. Assessment of static positioning accuracy using low-cost smartphone GPS devices for geodetic survey points' determination and monitoring. Appl Sci 2020;10:5308.
- 10. Paziewski J, Fortunato M, Mazzoni A, Odolinski R. An analysis of multi-GNSS observations tracked by recent android smartphones and smartphone-only relative positioning results. Measurement 2021;175:109162.
- 11. Sharma H, Bochkati M, Lichtenberger C, Pant T, Darugna F, Wubbena JB. Smartphone-based GNSS positioning. Today and tomorrow. New Jersey, USA: Richard Fischer, Inside GNSS Media LLC, in Red Bank; 2021.
- 12. Hamza V, Stopar B, Oskar S, Prešeren P. Recent advances and applications of low-cost GNSS receivers: a review. GPS Solut 2025:29:1-17.

- 13. Sun W, Li Y, Duan S. Xiaomi Mi 8 smartphone GNSS data quality analysis and single-frequency RTK positioning performance evaluation. IET Radar, Sonar Navig 2020;14:1410-16.
- 14. Dabove P, Di Pietra V. Single-baseline RTK positioning using dual-frequency GNSS receivers inside smartphones. Sensors 2019;19:4302.
- 15. Jiang Y, Gao Y, Ding W, Liu F, Gao Y. An improved ambiguity resolution algorithm for smartphone RTK positioning. Sensors
- 16. Odolinski R, Teunissen PJ. An assessment of smartphone and low-cost multi-GNSS single-frequency RTK positioning for low, medium and high ionospheric disturbance periods. J Geodesy
- 17. Li Y, Mi J, Xu Y, Li B, Jiang D, Liu W. A robust adaptive filtering algorithm for GNSS single-frequency RTK of smartphone. Remote Sens 2022:14:6388.
- 18. Shinghal G, Bisnath S. Conditioning and PPP processing of smartphone GNSS measurements in realistic environments. Satell
- 19. Aggrey J, Bisnath S, Naciri N, Shinghal G, Yang S. Multi-GNSS precise point positioning with next-generation smartphone measurements. J Spat Sci 2020;65:79-98.
- 20. Li Z, Wang L, Wang N, Li R, Liu A. Real-time GNSS precise point positioning with smartphones for vehicle navigation. Satell Navig 2022;3:19.
- 21. Wang L, Li Z, Wang N, Wang Z. Real-time GNSS precise point positioning for low-cost smart devices. GPS Solut 2021;
- 22. Hu J, Li P, Bisnath S. Towards GNSS ambiguity resolution for smartphones in realistic environments: characterization of smartphone ambiguities with RTK, PPP, and PPP-RTK. In: Proceedings of the 36th international technical meeting of the satellite division of the institute of navigation (ION GNSS+ 2023). Denver, Colorado: 2023:2698 – 711 pp.
- 23. Wen Q, Geng J, Li G, Guo J. Precise point positioning with ambiguity resolution using an external survey-grade antenna enhanced dual-frequency android GNSS data. Measurement 2020:157:107634.
- 24. Gao Y, Zhang Y, Lyu Z. A PPP-RTK approach to mass-market applications. Int Arch Photogramm Remote Sens Spat Inf Sci 2023;XLVIII-1/W1-2023:151-3.
- 25. Cellmer S, Wielgosz P, Rzepecka Z. Modified ambiguity function approach for GPS carrier phase positioning. J Geodesy 2010;84:267-75.
- 26. Kwaśniak D, Cellmer S, Nowel K. Schreiber's differencing scheme applied to carrier phase observations in the MAFA method.

- In: 2016 baltic geodetic congress (BGC geomatics). Gdansk, Poland; 2016:197-204 pp.
- 27. Cellmer S, Nowel K, Kwaśniak D. Optimization of a grid of candidates in the search procedure of the MAFA method. In: Environmental engineering, proceedings of the international conference on environmental engineering. ICEE; 2017, vol 10:1-7
- 28. Gao M, Liu G, Wang S, Xiao G, Zhao W, Lv D. Research on tightly coupled multi-antenna GNSS/MEMS single-frequency single-epoch attitude determination in urban environment. Remote Sens 2021;13:2710.
- 29. Zhu H, Xia L, Li Q, Xia J, Cai Y. IMU-aided precise point positioning performance assessment with smartphones in GNSS-degraded urban environments. Remote Sens 2022;14:4469.
- 30. Yi D, Naciri N, Bisnath S. Precise positioning utilizing smartphone GNSS/IMU integration with the combination of galileo high accuracy service (HAS) corrections and broadcast ephemerides. GPS Solut 2024;28:140.
- 31. Wang J, Shi C, Zheng F, Yang C, Liu X, Liu S, et al. Multi-frequency smartphone positioning performance evaluation: insights into A-GNSS PPP-B2b services and beyond. Satell Navig 2024;5:25.
- 32. Teunissen P, Kleusberg A. GPS for geodesy. Berlin, Heidelberg, New York: Springer-Verlag; 1998.
- 33. Kwaśniak D, Cellmer S, Nowel K. Precise positioning in Europe using the galileo and GPS combination. In: Proceedings of the international conference on environmental engineering. ICEE. Vilnius: Vilnius Gediminas Technical University Press; 2017, vol 10.
- 34. Cellmer S, Nowel K, Kwaśniak D. The new search method in precise GNSS positioning. IEEE Trans Aero Electron Syst 2018;54:404-15.
- 35. Xu P. Voronoi cells, probabilistic bounds, and hypothesis testing in mixed integer linear models. IEEE Trans Inf Theor 2006;52:3122-38.
- 36. Teunissen P, De Jonge P, Tiberius C. The LAMBDA method for fast GPS surveying. In: International symposium "qps technology applications". Bucharest, Romania; 1995.
- 37. Cellmer S, Nowel K, Fischer A. A search step optimization in an ambiguity function-based GNSS precise positioning. Surv Rev
- 38. Kim B, Kim J, Kee C, Yu S, Kim J. Analysis of RTK positioning accuracy using antenna calibrated commercial Samsung smartphone. In: Proceedings of the 2023 international technical meeting of the institute of navigation. Long Beach, California; 2023:611 – 23 pp.
- 39. Uradziński M, Bakuła M. Achieving centimeters-level GPS positioning accuracy using a smartphone for mapping applications. Int Arch Photogram Remote Sens Spat Inf Sci 2023;48:525-9.